Journal of Applied Mechanics and Technical Physics, Vol. 40, No. 2, 1999

NUMERICAL STUDY OF FLOWS OF REACTING COMPOSITE MIXTURES

A. V. Fedorov and V. M. Fomin

UDC 662.612.32

A distributed mathematical model is proposed to describe a flow of a mixture of gases, fine particles of a reacting metal, and droplets of a hydrocarbon fuel. The heterogeneous chemical reaction of low-temperature oxidation of the metal, the homogeneous oxidation reaction of the reacting vaporized liquid fuel, and the difference in phase velocities and temperatures are taken into account. It is shown that this model can be used to describe the problems of detonation in a mixture of a reacting gas and reacting solid particles, and the problems of ignition of a mixture of aluminum particles and tridecane droplets.

1. Equations of Mechanics of Heterogeneous Media for Describing the Motion of a K-mixture. We consider a mixture consisting of oxygen (subscript 11), metal particles (22), and a solid oxide (23), which is called a K-mixture. A chemical reaction proceeds in this mixture, which obeys the stoichiometric relationship

$$\nu_{11}^1 + \nu_{22}^1 = \nu_{23}^1.$$

Here $\nu_{ij}^1 = \tilde{\nu}_{ij}^1 \mu_{ij}$, $\tilde{\nu}_{ij}^1$ and μ_{ij} are the stoichiometric coefficients and molecular masses of the corresponding phases and components. This mixture contains also the droplets of an inflammable liquid (the subscript 32), its combustible vapors (12), gaseous products of combustion of fuel vapor (13), and the inert phase (14), which burn in accordance with the stoichiometric relationship

$$\nu_{11}^2 + \nu_{22}^2 = \nu_{23}^2.$$

The continuity equations for the gaseous and condensed components of the mixture have the form

$$\begin{gathered} \partial_t \rho_1 + \partial_x \rho_1 u_1 = -\nu_{11}^1 w^1 + w_v \equiv \bar{\nu}_{22}^1 w^1 + w_v = w_1, \\ \partial_t \rho_2 + \partial_x \rho_2 u_2 = -(\bar{\nu}_2^1 w^1 + w_v) = w_2 = -w_1, \end{gathered} \tag{1.1}$$

where $\rho_1 = m_1(\rho_{11}^0 + \rho_{12}^0 + \rho_{13}^0 + \rho_{14}^0)$ and $\rho_2 = m_{22}\rho_{22}^0 + m_{23}\rho_{23}^0 + m_{32}\rho_{32}^0$ are the virtual densities and ρ_{ij}^0 are the intrinsic densities of the gaseous and condensed phases, $\partial_t = \partial/\partial t$, and $\partial_x = \partial/\partial x$. The kinetic equations and the conservation equations of the number of particles and droplets (n_2 and n_3) can be represented as

$$\rho_1 \frac{d_1\xi_{11}}{dt} = (1-\xi_{11})\bar{\nu}_{22}^1 w^1 - \nu_{11}^2 w^2 - \xi_{11} w_v, \quad \rho_1 \frac{d_1\xi_{12}}{dt} = -\xi_{12}\bar{\nu}_{22}^1 w^1 - \nu_{11}^2 w^2 + w_v(1-\xi_{12}),$$

$$\rho_1 \frac{d_1\xi_{13}}{dt} = -\xi_{13}\bar{\nu}_{22}^1 w^1 + \nu_{13}^2 w^2 - w_v\xi_{13}, \qquad \rho_1 \frac{d_1\xi_{14}}{dt} = -\xi_{14}\bar{\nu}_{22}^1 w^1 - w_v\xi_{14},$$

$$\rho_2 \frac{d_2\xi_{22}}{dt} = (-\nu_{22}^1 + \bar{\nu}_{22}^1\xi_{22})w^1 + w_v\xi_{22}, \tag{1.2}$$

$$\rho_2 \frac{d_2\xi_{23}}{dt} = (\nu_{23}^1 + \bar{\nu}_{22}^1\xi_{23})w^1 + w_v\xi_{23}, \qquad \rho_2 \frac{d_2\xi_{32}}{dt} = \bar{\nu}_{22}^1\xi_{32}w^1 + w_v(\xi_{32}-1),$$

$$\partial_t n_j + \partial_x n_j u_2 = 0, \qquad j = 2, 3.$$

Here $d_i/dt = \partial_t + u_i\partial_x$ $(i = 1, 2)$ and $\xi_{ij} = \rho_{ij}/\rho_i$.

Institute of Theoretical and Applied Mechanics, Siberian Division, Russian Academy of Sciences, Novosibirsk 630090. Translated from Prikladnaya Mekhanika i Tekhnicheskaya Fizika, Vol. 40, No. 2, pp. 128–136, March–April, 1999. Original article submitted August 21, 1998.

The equations of motion of the phases and components are

$$\begin{aligned}\partial_t(\rho_1 u_1) + \partial_x(\rho_1 u_1^2 + m_1 p) &= p\partial_x m_1 + (\bar{\nu}_{22}^1 w^1 + w_v)u_2 + f,\\ \partial_t(\rho_2 u_2) + \partial_x(\rho_2 u_2^2 + m_2 p) &= p\partial_x m_2 - (\bar{\nu}_{22}^1 w^1 + w_v)u_2 - f.\end{aligned} \tag{1.3}$$

Here m_i and m_{ij} are the volume concentrations of the phases, f is the force of interaction between the phases, and p is the pressure in the mixture.

The energy equations for the phases and components are

$$\begin{aligned}&\partial_t(\rho_1 E_1) + \partial_x(\rho_1 u_1 E_1 + m_1 p u_1)\\ &= -p\partial_t m_1 - (\bar{\nu}_{22}^1 w^1 + w_v)\Big(-x_2 + i_1 + \frac{u_2^2}{2}\Big) + y w_v + q_1 + f(\beta u_1 + \bar{\beta} u_2),\\ &\partial_t(\rho_2 E_2) + \partial_x(\rho_2 u_2 E_2 + m_2 p u_2)\\ &= -p\partial_t(m_{22} + m_{23} + m_3) + (\bar{\nu}_{22}^1 w^1 + w_v)\Big(-x_2 + i_2 - \frac{u_2^2}{2}\Big) - y w_v + q_2 - f(\beta u_1 + \bar{\beta} u_2),\end{aligned} \tag{1.4}$$

where x_i and y are the desired accommodation coefficients, which are determined from the condition of conservation of the total energy in the K-mixture:

$$x_1 = i_1 - i_{11} - \alpha q_1, \quad x_2 = -i_2 + i_{11} + \alpha q_1, \quad y = x_1 + i_{12} - i_1 - |\lambda| L.$$

Here α is the fraction of heat released in the gas because of the heterogeneous chemical reaction, λ is the fraction of heat of droplet vaporization L, which is consumed from the gaseous phase, i_{ij} is the enthalpy of the ijth component, $q_i = q_i^*/\bar{\nu}_{22}^1$, q_i^* is the heat of the chemical reaction, which is determined by the standard manner, and E_i is the total energy of the phases.

The system is closed by the thermal equation of state and the geometric equality

$$p = p(\rho_1, \rho_2, T_1, \xi_{1j}, \xi_{2j}), \qquad R^3 - R_0^3 = a(r_2^3 - r_{20}^3). \tag{1.5}$$

Here $R = r_2 + h$, where r_2 is the particle radius and h is the oxide film thickness, and a is a certain constant, which depends on the stoichiometric coefficients.

We determine the source terms

$$w_1 = -\frac{3\rho_{22}}{r_2 \nu_{22}^1}\frac{d_2 r_2}{dt}, \qquad w_v = -\frac{3\rho_{32}}{r_3}\frac{d_2 r_3}{dt},$$

where the changing rates of the particle and droplet radii $d_2 r_i/dt$ are assumed to be known functions of the parameters of state.

Thus, system (1.1)–(1.5) is closed relative to 19 functions (virtual densities, velocities, temperatures, pressure, radii and the number of droplets and particles, and the oxide film thickness).

We describe two problems of mechanics of reacting heterogeneous media, which were solved using the model proposed above.

2. Detonation in a Mixture of Reacting Gases and Reacting Particles. We consider the specific case of the K-mixture consisting of reacting gaseous components and fine solid particles capable of reaction. The initiation of detonation in such a mixture can cause the propagation of detonation regimes with a two-front structure. These types of flow were experimentally observed by Veyssiere and Manson [3] who later developed some mathematical models for the description of the two-front detonation in the steady approximation. The problem of description of two-front regimes in similar mixtures was solved for the first time by Kazakov et al. [4] within the framework of both one-dimensional steady and unsteady approaches of mechanics of reacting heterogeneous media. Since this paper was published in small circulation and, judging from publications in this field of science, has not lost its novelty, it seem reasonable to present here some of its results.

System (1.1)–(1.5), which describes the flow of a gas mixture in the case of integral kinetics and the

specific type of the K-mixture, takes the following form:

$$\partial_t\rho_1 + \partial_x(\rho_1 u_1) = J, \quad \partial_t\rho_2 + \partial_x(\rho_2 u_2) = -J, \quad \partial_t(\rho_1 u_1) + \partial_x(\rho_1 u_1^2) + m_1\partial_x p = f + Ju_2,$$
$$\partial_t(\rho_2 u_2) + \partial_x(\rho_2 u_2^2) + m_2\partial_x p = -f - Ju_2, \quad \partial_t(\rho_2 e_2) + \partial_x(\rho_2 u_2 e_2) = q - Je_2,$$
$$\partial_t(\rho_1 E_1 + \rho_2 E_2) + \partial_x(\rho_1 u_1 E_1 + \rho_2 u_2 E_2 + p(u_1 m_1 + u_2 m_2)) = 0,$$
$$\frac{d_2(d)}{dt} = -p^\alpha K(d - d_k), \qquad K = \begin{cases} 0, & T_2 < T_{2s}, \\ K_0, & T_2 < T_{2s}, \end{cases}$$
$$\partial_t(\rho_1\beta) + \partial_x(\rho_1 u_1\beta) = -\rho_1\beta b\exp\Big(-\frac{E}{RT_1}\Big), \qquad b = \begin{cases} 0, & T_1 < T_{1s}, \\ b_0, & T_1 > T_{1s}, \end{cases} \tag{2.1}$$
$$n = \frac{6m_2}{\pi d^3}, \quad m_1 + m_2 = 1, \quad p = \rho_{11}RT_1, \quad \rho_{22} = r = \text{const}, \quad \rho_i = m_i\rho_{ii},$$
$$e_1 = c_{v1}T_1 + \beta Q_1, \quad e_2 = c_2 T_2 + Q_2, \quad E_i = e_i + \frac{u_i^2}{2}, \quad J = -\frac{3\rho_2}{d}\frac{d_2(d)}{dt},$$
$$f = \frac{n\pi d^2}{8} C_D\rho_{11}|u_1 - u_2|(u_1 - u_2), \qquad q = n\pi s\lambda_1 \mathrm{Nu}\,(T_1 - T_2).$$

The parameters marked by the subscripts 1 and 2 refer to the gas and particles, respectively. The quantity β indicates the fraction of the nonreacted combustible substance, i.e., the chemical reaction with the activation energy E ends at $\beta = 0$. It is seen that the burning of the gaseous phase follows Arrhenius-type kinetics. The combustion of particles obeys the kinetic equation, which allows incomplete combustion (d_k is the diameter of an incompletely burned particle). The ignition delay is no longer observed for the particles when their temperature reaches T_{2s}, after which the combustion process described by the above-mentioned equation begins. The combustion in the gas begins when its temperature equals T_{1s}. The heat of combustion of the gas and particles is denoted by Q_1 and Q_2, respectively. The following parameters of the mixture were chosen: $\gamma = 1.4$, $c_2 = 716$ J/(kg·K), $c_{v1} = 710$ J/(kg·K), $Q_1 = 1.2 \cdot 10^6$ J/kg, $b = 2 \cdot 10^2$ sec^{-1}, $E/R = 700$ K, $\rho_{22} = 1960$ kg/m^3, $\rho_{11,0} = 1$ kg/m^3, $m_{20} = 10^{-3}$, $d_k = 50$ μm, $T_0 = 300$ K, $\mu = 1.7 \cdot 10^{-5}$ kg/(m·sec), and $\lambda = 2.47 \cdot 10^{-2}$ kg·m/(sec^3·K).

For the coefficients of force and thermal interaction, we used the simplest relationships $C_D = 24/\mathrm{Re}$ and $\mathrm{Nu} = 2$, which significantly decrease the computation time and retain the main features of the flow. Here Re and Nu are the Reynolds and Nusselt numbers.

The effect of the physicochemical parameters of the components of the mixture on the detonation wave (DW) structure was studied in the calculations. It was studied, in particular, how the detonation wave structure was changed by varying the combustion heat of the particles within a certain range. Figure 1a shows the distribution of the DW Mach number $\mathrm{M}_1 = (u_1 - D)/c_f$ along the abscissa axis, which was calculated in the steady approximation of system (2.1). The wave velocity in the self-sustained supersonic regime of normal detonation is $D_J = 1166.657$ m/sec. A lower wave velocity leads to flow choking and a higher velocity leads to strong detonation waves with a subsonic flow at the final point relative to the equilibrium speed of sound. The flow behind the Chapman–Jouguet (CJ) point determined from the frozen speed of sound c_f can be both subsonic and supersonic. Mathematically, this is caused by a saddle singular point of the mathematical model. For a weak detonation regime, the sign of the action on the mixture flow is changed at this point: the heat is extracted from the flow. Because of that, the supersonic flow continues to accelerate, and the particle temperature remains lower than the gas temperature. Finally, the particles are heated to the ignition temperature T_{1s}. This moment is marked by an inflection of curve 1 in Fig. 1a. The heat of particle combustion enters the flow, and the sign of effective action is changed, which leads to flow deceleration. The energy released during combustion is sufficient for the flow to remain supersonic and reach an equilibrium state. Such a flow is self-sustained, since the rarefaction wave cannot catch the Chapman–Jouguet plane propagating with a supersonic velocity.

If the mixture flow is sustained by a subsonic piston, the flow pattern is different. A shock wave (SW)

arises in the supersonic flow region, and its downstream position cannot be determined unambiguously (curves 2 and 3 in Fig. 1a) if the wave velocity equals D_J. A strong regime is observed for wave velocity greater than D_J.

If the heat of combustion of the particles exceeds a certain critical value Q^*, supersonic flow choking occurs behind the first CJ point because of excessive heat addition from particle combustion, which makes it necessary to introduce a strong discontinuity behind the first CJ point. It is also possible to increase the DW velocity relative to D_J (D_J is understood here as the wave velocity corresponding to the stage of gas combustion). Figure 1b shows the DW Mach number distribution for $Q_2 = 3.2 \cdot 10^5$ m^2/sec^2 $> Q^*$. Curve 1 corresponds to supersonic flow choking in the case where the second SW is absent, and curve 2 refers to the second eigendirection at the first singular point. The flow is sustained by a subsonic piston, i.e., a strong detonation regime is observed. Curve 3 corresponds to flow with the second SW at the point $\xi = 0.124$. All these cases are characterized by the fact that the combustion of particles does not lead to the transition through the speed of sound. If we increase the abscissa of the SW position, flow choking arises in the wave structure (curves 5 and 6). This means that there exists a motion pattern of the medium where the second CJ point (curve 4) lies in the interval between strong and choked flows. The position of the second SW is the free parameter of the problem and, for $\xi = \xi_* = 0.190184$, determines the structure of the detonation wave with two CJ points. This weak detonation flow has a supersonic final state.

We consider a flow with a small displacement of the second SW from the position ξ_* toward lower ξ. In this case, the detonation wave becomes strong; hence, if it is not supported by a piston, it is attenuated by the rarefaction wave. The second SW lags behind the first one until it occupies the position $\xi = \xi_*$. If we shift the second SW toward higher values on the abscissa axis, this leads to flow choking, i.e., to emergence of compression waves, which amplify the SW until it occupies a stable position $\xi = \xi_*$. Our calculations show that it is possible to find such a point within the interval $Q^* < Q_2 < Q^{**}$.

Figure 1c shows the DW Mach number distribution for the case $Q_2 = 5 \cdot 10^5 > Q^{**}$. In this case, the first CJ point disappears in the normal detonation regime. Gas combustion leads to a strong detonation flow, which is sustained by combustion of particles. The wave velocity in the detonation regime increases with increasing Q_2 for $Q_2 > Q^{**}$, in contrast to the intermediate range of heat values where the DW velocity is independent of the heat of particle combustion. For this value of Q_2, the DW velocity was chosen in the standard manner, i.e., by the method of iterations under the condition of continuous transition through a saddle singularity of the system of ordinary differential equations of the mathematical model of motion of the mixture. In particular, the eigenvalue of the model $D_{\mathrm{CJ}} = 1241.2336$ m/sec was found, which corresponds to curve 2 in Fig. 1c; curve 1 refers to flow with the velocity $D < D_{\mathrm{CJ}}$ at which the flow choking occurs. Finally, the propagation of a strong regime sustained by a subsonic piston is observed for $D > D_{\mathrm{CJ}}$ (curve 3).

Figure 2 shows the pressure distributions along the DW front. Curve 1 corresponds to the first interval in Q_2 when the self-sustained detonation regime ensures gas combustion ($Q_2 < Q^*$). Curve 2 refers to the two-front regime of CJ detonation where the flow contains the leading frozen and internal shock waves ($Q^* < Q_2 < Q^{**}$). This type of flow is characterized by interaction of heat release in both phases. Curve 3 corresponds to a detonation flow with significant heat release in the discrete phase $Q_2 > Q^{**}$. The position of the CJ plane is marked by a closed circle and the ignition point by an open circle.

The parameters Q^* and Q^{**} are determined by the kinetic parameters of the medium. In each particular case, these parameters are found from numerical calculations. The effect of heat release of the particles on the flow structure is described above. The influence of other parameters, such as the relaxation times of nonequilibrium processes, can be also studied. It should be expected that the types of detonation flows remain the same.

To examine the stability of the structure of different DW types, we also used the pseudo-transient method, which can be interpreted as the solution of the problem of DW initiation. The mathematical formulation of this problem corresponds to the classical problem of decay of an arbitrary discontinuity in a combustible gas mixture for the solution vector $\Phi(\rho_1, \rho_2, u_1, u_2, T_1, T_2, d)$ of the system of nonstationary equations (2.1). The gas temperature in the high-pressure chamber was assumed to be higher than the ignition temperature.

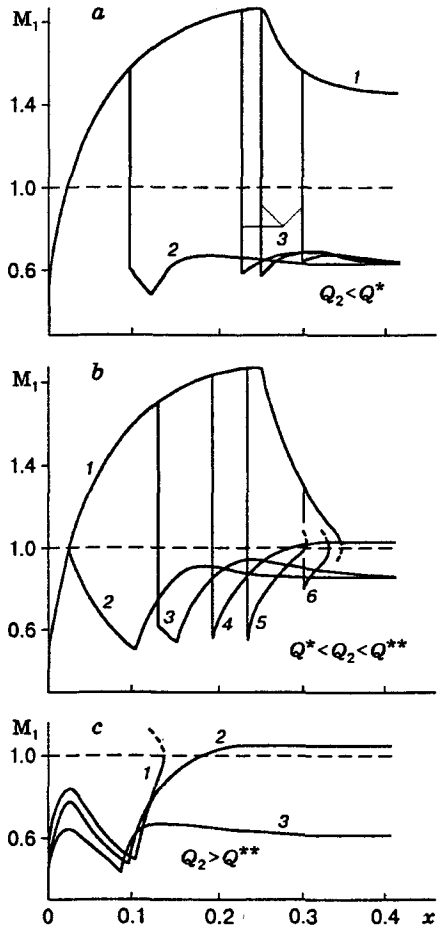

Fig. 1

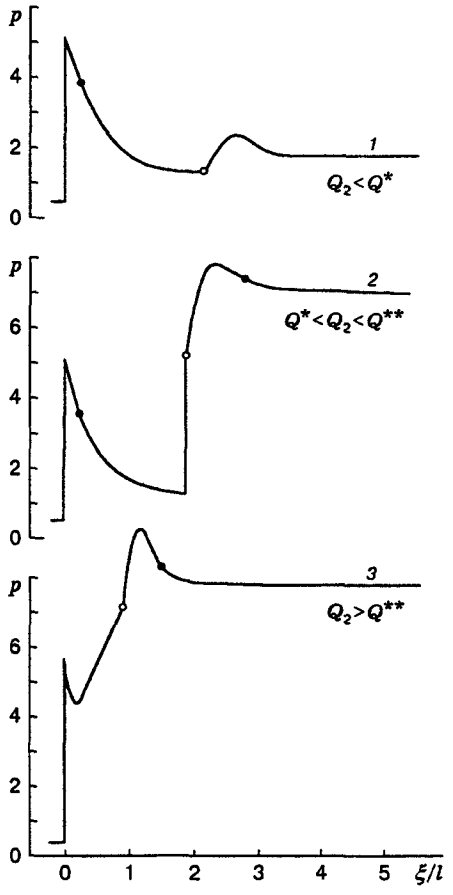

Fig. 2

The calculation results for the case of two-front detonation [$Q_2 = 3.5 \cdot 10^5 \in (Q^*, Q^{**})$] are shown in Fig. 3a. A comparison of nonstationary and stationary (see Fig. 2, curve 2) pressure profiles p of the gas reveals their qualitative and quantitative agreement. Figure 3b shows the calculated pressure profile for $Q_2 = 5 \cdot 10^5$, where a one-front regime similar to that plotted in Fig. 2 (curve 3) is observed. The third type of detonation flow is initiated in a similar manner. Note that the calculations were performed using the coarse particle method adapted for calculation of reacting two-velocity two-temperature mixtures.

3. Thermal Explosion in a Mixture of Droplets and Solid Particles. We consider a K-mixture consisting of droplets of a hydrocarbon fuel (tridecane or isooctane) and particles of a reacting metal (Al) dispersed in a volume filled by a gas mixture, which consists of an oxidizer, vaporized fuel, and gaseous products of reaction. The mathematical model of this phenomenon and its verification for the specific case of tridecane ignition behind the reflected SW front in oxygen are presented [5]. Some calculation data, which refer to the behavior of the system parameters in time, are given below.

The calculations were performed both for small particles with radius 2 μm and for large particles with radius 100 μm. The total mass of these droplets corresponded to the mass of a large drop of tridecane with radius no more than 1.5 mm, which experienced splitting in a passing SW in experiments performed at the Institute of Theoretical and Applied Mechanics of the Siberian Division of the Russian Academy of Sciences [6].

The calculation results are shown in the subsequent figures, where Y_1 is the relative mass concentration of tridecane microdroplets, C_{20} and r_{20} are the initial mass and radius of these droplets, and T_0 and p_0 are

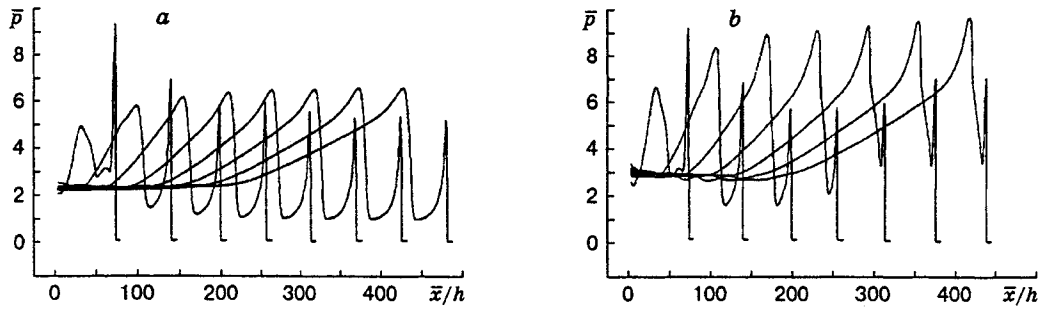

Fig. 3

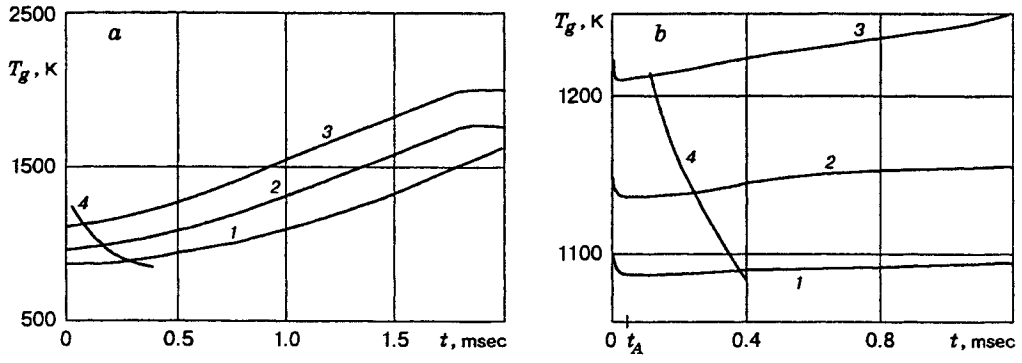

Fig. 4

the temperature and pressure behind the reflected SW front at the time when the splitting of a large droplet is finished.

For $p_0 = 1.01 \cdot 10^5$ and $0.505 \cdot 10^5$ Pa, Fig. 4 shows the calculated temperature of the mixture T_g for the initial values of 900, 1000, and 1150 K (curves 1–3) and the experimental ignition delays versus the ambient temperature (curves 4). It is seen that the temperature of the mixture decreases in the period of ignition at low pressures. This can be caused by an insufficient rate of heat release in the chemical reaction. The curves of the delay of the appearance of visible flame, i.e., the ignition delay $t_{\text{ign}}(T_0)$, which correspond to the set of constants that characterize the kinetic law of oxidation of microdroplets, can be found [5, Fig. 1]. The calculated and experimental curves are in good agreement.

According to calculations, the combustion acquires a deflagration-like character as the pressure decreases. In particular, a comparison of the gas temperature curves in Fig. 4 shows that, though the temperature increase is much weaker in the case of lower pressure, the combustion and, hence, the flame are stable. For $p_0 < 0.505 \cdot 10^5$ Pa, the conducted calculations reveal the decay of combustion; this is associated with the decrease in the reaction rate in the gas, which is in quadratic proportion to the pressure decrease. In turn, the latter circumstance is connected with a proportional dependence of the molar concentration of the oxidizer on pressure.

The size of the fuel microdroplets affects the ignition process. Thus, it is seen in Fig. 4b that there is a dramatic decrease in the gas temperature in the time interval $(0, t_A)$, which is mainly related to heat losses on vaporization of liquid particles. The speed of gas temperature decrease caused by this effect is proportional to the total area of the surface of microdroplets; therefore, the total mass of the clouds of fuel microparticles being equal, those with smaller mean dimensions have greater total surfaces of vaporization, which leads to a decrease in the gas temperature. For low pressures, i.e., an insufficient molar concentration of the oxidizer, this decrease hinders the ignition process.

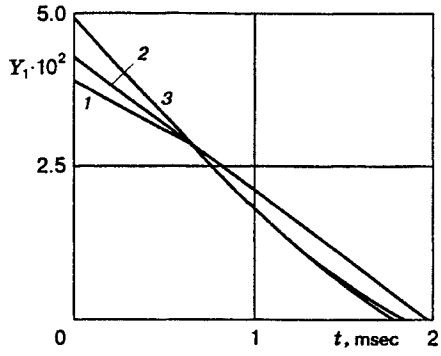

Fig. 5

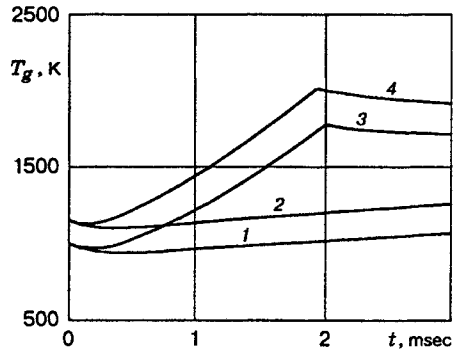

Fig. 6

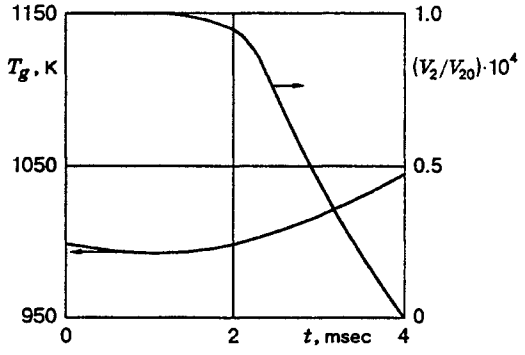

Fig. 7

Figure 5 shows the distribution of the mass concentration of tridecane vapor for $p_0 = 1.01 \cdot 10^5$ Pa. Curves 1–3 correspond to the initial values of the ambient temperature, as in Fig. 4a. It was stated in experiments [6] that the total time of combustion of tridecane vapor (i.e., the presence of visible flame) under these conditions is at least 1.5 msec, which is in good agreement with the calculated data on the total time of combustion of the droplets. It was also noted [6] that, for pressures behind the SW of about 101.3 kPa, the combustion process is accompanied by intense glowing, which appears in one or several regions and rapidly propagates over the combustible mixture. The calculated pattern of gas temperature variation during combustion supports qualitatively this idea.

The complex pattern of ignition, which depends on the size of microdroplets, is characterized by the complex temperature functions shown in Figs. 4 and 6. In Fig. 6, the size of microdroplets was 10 μm (cf. 2 μm in Fig. 4). For $p_0 = 1.01 \cdot 10^5$ Pa, curves 1 and 2 correspond to $T_0 = 1000$ and 1150 K, respectively; for $p_0 = 0.505 \cdot 10^5$ Pa, curves 3 and 4 correspond to $T_0 = 1000$ and 1150 K respectively. The initial mass of the droplets is identical for all the cases (see Figs. 4 and 6) and equal to $1.131 \cdot 10^{-5}$ kg. An analysis of the calculated data shows that the increase in the size of microdroplets, their total mass being the same, leads, on the one hand, to a smaller ignition induction time and, on the other hand, to a greater total time of combustion of the mixture. The first effect is related to lower heat losses on vaporization, and the second phenomenon is associated with a lower rate of increasing concentration of the fuel vapor.

Figure 7 shows typical curves of the gas temperature and droplet volume at times preceding the complete vaporization of the droplet. The lower curve corresponds to the gas temperature and the upper curve refers to the relative volume. Here $p_0 = 1.01 \cdot 10^5$ Pa, $T_0 = 1000$ K, $r_{20} = 10^{-5}$ m, and $G_{20} = 1.131 \cdot 10^{-5}$ kg. The calculated mean rate of vaporization is $K = 10^{-6}$ m^2/sec. This result is close to that observed in experiments [7].

Thus, the mathematical model proposed in this paper describes the flow of a mixture of gases, liquid particles, and solid particles with account of hetero- and homogeneous chemical reactions, nonequilibrium vaporization of the liquid phase, and the difference in phase temperatures and velocities.

Based on this model, in the problem of detonation in a mixture of reacting gases and particles, possible detonation flows of the mixture in the form of one- and two-front regimes are classified depending on the heat release in the phases.

In the problem of ignition of a K-mixture, it is shown that this mathematical model adequately describes experimental results on the combustion time of tridecane vapor and vaporization time of a liquid droplet.

This work was supported by the Russian Foundation for Fundamental Research (Grant No. 96-01-01886).

REFERENCES

1. A. V. Fedorov, "Ignition of gas mixture in the regime of interacting continua," *Fiz. Goreniya Vzryva*, **34**, No. 4, 95–102 (1998).
2. Yu. A. Gosteev, A. V. Fedorov, and V. M. Fomin, "Theory of motion of a mixture of gas/liquid droplets with regard for ignition," *Dokl. Ross. Akad. Nauk*, **363**, No. 5, 623–625 (1998).
3. B. Veyssiere and N. Manson, "Sur l'existaese d'un second front de detonation des melanges biphasiques hydrogene–oxygene–azote particules d'aluminum," *Comp. Rend. Acad. Sci.*, **295**, Part II, 335–338 (1982).
4. Yu. V. Kazakov, A. V. Fedorov, and V. M. Fomin, "Detonation dynamics of gas mixtures," Preprint No. 23-87, Inst. of Theor. and Appl. Mech., Sib. Div., Russian Acad. of Sci., Novosibirsk (1987).
5. A. V. Fedorov, V. M. Fomin, and S. I. Volkov, "Mathematical model of ignition of an aerosuspension of liquid fuel and solid particles," *Fiz. Goreniya Vzryva*, **33**, No. 3, 86–94 (1997).
6. A. N. Papyrin, V. M. Boiko, S. V. Poplavskii, et al., "Experimental study of ignition and combustion of liquid fuel droplets in reflected shock waves," Report No. 1579, Inst. of Theor. and Appl. Mech., Sib. Div., Russian Acad. of Sci., Novosibirsk (1985).
7. V. V. Pomerantsev (ed.), *Fundamentals of the Practical Theory of Combustion* [in Russian], Energoizdat, Leningrad (1983).